JACS ARTICLES

Published on Web 04/23/2009

Enantiomer-Selective and Helix-Sense-Selective Living Block Copolymerization of Isocyanide Enantiomers Initiated by Single-Handed Helical Poly(phenyl isocyanide)s

Zong-Quan Wu,[†,‡] Kanji Nagai,[†,‡] Motonori Banno,[†] Kento Okoshi,[‡,§] Kiyotaka Onitsuka,[||,⊥] and Eiji Yashima*[,†,‡]

Department of Molecular Design and Engineering, Graduate School of Engineering, Nagoya University, Chikusa-ku, Nagoya 464-8603, Japan, Yashima Super-structured Helix Project, Exploratory Research for Advanced Technology (ERATO), Japan Science and Technology Agency (JST), Japan, and The Institute of Scientific and Industrial Research, Osaka University, 8-1 Mihogaoka, Ibaraki, Osaka 567-0047, Japan

Received January 4, 2009; E-mail: yashima@apchem.nagoya-u.ac.jp

Abstract: Rigid-rodlike right (*P*)- and left (*M*)-handed helical polyisocyanides (*P*-poly-L-**1** and *M*-poly-L-**1**) prepared by the living polymerization of an enantiomerically pure phenyl isocyanide bearing an L-alanine pendant with a long *n*-decyl chain (L-**1**) with the μ-ethynediyl Pt−Pd catalyst were found to block copolymerize L-**1** and D-**1** in a highly enantiomer-selective manner while maintaining narrow molecular weight distributions. The *M*-poly-L-**1** preferentially copolymerized L-**1** over the antipode D-**1** by a factor of 6.4−7.7, whereas the D-**1** was preferentially copolymerized with *P*-poly-L-**1** composed of the same L-**1** units, but possessing the opposite helicity by a factor of 4.0. Circular dichroism and high-resolution atomic force microscopy revealed that the enantiomer-selective block copolymerizations proceed in an extremely high helix-sense-selective fashion, and the preformed helical handedness determines the overall helical sense of the polyisocyanides irrespective of the configuration of the monomer units of the initiators during the block copolymerizations. The block copolymers are rigid-rod helical polymers with a narrow molecular weight distribution and exhibit a lyotropic smectic liquid crystalline phase.

Introduction

The helix is the prevalent structural motif for biological polymers and plays key roles in their sophisticated functions, such as chiral recognition, asymmetric catalysis, and replication. Since the discovery of biological helices, a large number of helical polymers[1] and oligomers (foldamers)[2] with a controlled helix-sense have been synthesized not only to mimic biological helices, but also to realize novel functions, but relatively few successful applications originating from a one-handed helicity have been reported for chiral separations and asymmetric catalysis.[1a,g,3] We now report a unique chiral recognition of a living polymer chain with a rigid single-handed helical conformation that preferentially copolymerizes one of the isocyanide enantiomers. The relatively high enantiomer selectivity was totally controlled by the one-handed helical structure of the growing polymer chains that can simultaneously control the helical sense of the block copolymer units in an almost perfect helix-sense selective manner (Figure 1). Atomic force microscopy (AFM) revealed unambiguous evidence for the helix-sense-selective living block copolymerization by direct observations of the molecular lengths as well as the helical conformations of the block copolymers.

The enantiomer-selective polymerization is a kind of kinetic resolution, closely related to the stereospecific reactions of enzymes, through which one enantiomer is preferentially polymerized over the antipode, giving an optically active polymer as well as an optically active unreacted monomer.[1a,4] Although a number of studies have been reported on the enantiomer-selective polymerizations of racemic monomers, including vinyl[5] and cyclic[6] monomers, the enantiomer selectivity was mostly attained by optically active catalysts or initiators. However, if the growing polymer chains could form a preferred-handed helical conformation, the macromolecular helicity would contribute to and/or enhance the enantiomer selectivity during the polymerization as demonstrated half a century ago for the

† Nagoya University.
‡ ERATO, JST.
§ Present address: Department of Organic and Polymeric Materials, Graduate School of Science and Engineering, Tokyo Institute of Technology, 2-12-1, Ookayama, Meguro-ku, Tokyo 152-8552, Japan.
|| Osaka University.
⊥ Present address: Department of Macromolecular Science, Osaka University, 1-1 Machikaneyama-cho, Toyonaka, Osaka 560-0043, Japan.

(1) For reviews: (a) Okamoto, Y.; Nakano, T. *Chem. Rev.* **1994**, *94*, 349–372. (b) Nolte, R. J. M. *Chem. Soc. Rev.* **1994**, *23*, 11–19. (c) Green, M. M.; Peterson, N. C.; Sato, T.; Teramoto, A.; Cook, R.; Lifson, S. *Science* **1995**, *268*, 1860–1866. (d) Pu, L. *Acta Polym.* **1997**, *48*, 116–141. (e) Srinivasarao, M. *Curr. Opin. Colloid Interface Sci.* **1999**, *4*, 370–376. (f) Green, M. M.; Park, J.-W.; Sato, T.; Teramoto, A.; Lifson, S.; Selinger, R. L. B.; Selinger, V. B.; Selinger, J. V. *Angew. Chem., Int. Ed.* **1999**, *38*, 3138–3154. (g) Nakano, T.; Okamoto, Y. *Chem. Rev.* **2001**, *101*, 4013–4038. (h) Cornelissen, J. J. L. M.; Rowan, A. E.; Nolte, R. J. M.; Sommerdijk, N. A. J. M. *Chem. Rev.* **2001**, *101*, 4039–4070. (i) Fujiki, M. *Macromol. Rapid Commun.* **2001**, *22*, 539–563. (j) Nomura, R.; Nakako, H.; Masuda, T. *J. Mol. Catal. A: Chem.* **2002**, *190*, 197–205. (k) Fujiki, M.; Koe, J. R.; Terao, K.; Sato, T.; Teramoto, A.; Watanabe, J. *Polym. J.* **2003**, *35*, 297–344. (l) Elemans, J. A. A. W.; Rowan, A. E.; Nolte, R. J. M. *J. Mater. Chem.* **2003**, *13*, 2661–2670. (m) Yashima, E.; Maeda, K.; Nishimura, T. *Chem.-Eur. J.* **2004**, *10*, 42–51. (n) Lam, J. W. Y.; Tang, B. Z. *Acc. Chem. Res.* **2005**, *38*, 745–754. (o) Lockmam, J. W.; Paul, N. M.; Parquette, J. R. *Prog. Polym. Sci.* **2005**, *30*, 423–452. (p) Aoki, T.; Kaneko, T.; Teraguchi, M. *Polymer* **2006**, *47*, 4867–4892. (q) Maeda, K.; Yashima, E. *Top. Curr. Chem.* **2006**, *265*, 47–88. (r) Rudick, J. G.; Percec, V. *New J. Chem.* **2007**, *31*, 1083–1096. (s) Yashima, E.; Maeda, K. *Macromolecules* **2008**, *41*, 3–12. (t) Kim, H.-J.; Lim, Y.-B.; Lee, M. *J. Polym. Sci., Part A: Polym. Chem.* **2008**, *46*, 1925–1935. (u) Pijper, D.; Feringa, B. L. *Soft Matter* **2008**, *4*, 1349–1372. (v) Yashima, E.; Maeda, K.; Furusho, Y. *Acc. Chem. Res.* **2008**, *41*, 1166–1180. (w) Rudick, J. G.; Percec, V. *Acc. Chem. Res.* **2008**, *41*, 1641–1652.

(2) For reviews: (a) Gellman, S. H. *Acc. Chem. Res.* **1998**, *31*, 173–180. (b) Hill, D. J.; Mio, R. J.; Prince, R. B.; Hughes, T. S.; Moore, J. S. *Chem. Rev.* **2001**, *101*, 3893–4011. (c) Brunsveld, L.; Folmer, B. J. B.; Meijer, E. W.; Sijbesma, R. P. *Chem. Rev.* **2001**, *101*, 4071–4097. (d) Sanford, A. R.; Gong, B. *Curr. Org. Chem.* **2003**, *7*, 1649–1659. (e) Huc, I. *Eur. J. Org. Chem.* **2004**, 17–29. (f) Hecht, S.; Huc, I. *Foldamers-Structure, Properties, and Applications*; Wiley-VCH: Weinheim, Germany, 2007.

(3) For reviews: (a) Okamoto, Y.; Yashima, E. *Angew. Chem., Int. Ed.* **1998**, *37*, 1020–1043. (b) Yashima, E. *J. Chromatogr., A* **2001**, *906*, 105–125. (c) Nakano, T. *J. Chromatogr., A* **2001**, *906*, 205–225. (d) Reggelin, M.; Doerr, S.; Klussmann, M.; Schultz, M.; Holbach, M. *Proc. Natl. Acad. Sci. U.S.A.* **2004**, *101*, 5461–5466.

10.1021/ja900036n CCC: $40.75

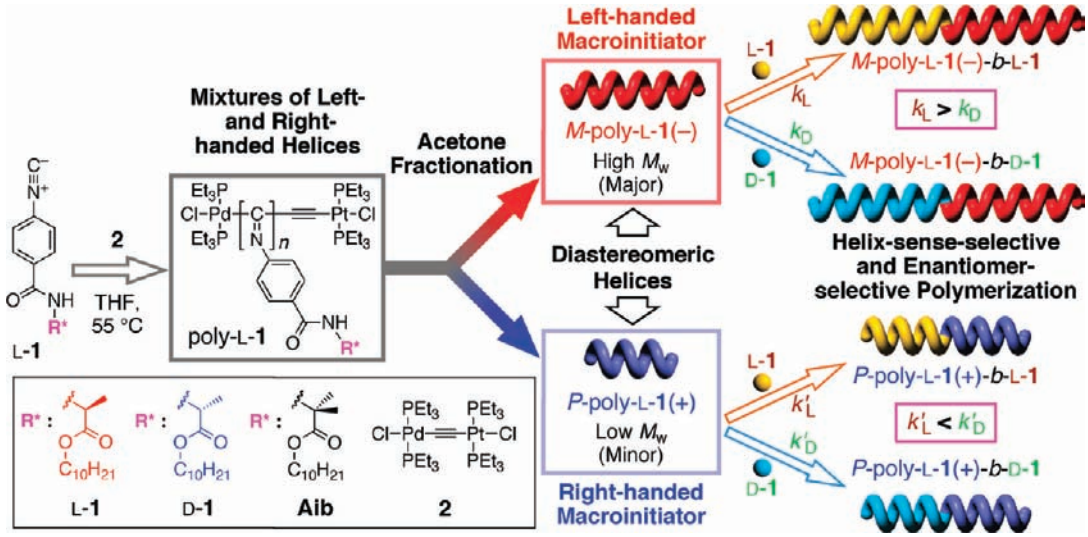

Figure 1. Schematic illustration of the helix-sense-selective living polymerization of L-**1** with μ-ethynediyl Pt−Pd complex (**2**), yielding a mixture of diastereomeric, right- and left-handed helical poly-L-**1**'s with different MWs and narrow MWDs, which can be further separated into the left-handed helical *M*-poly-L-**1**(−) and right-handed helical *P*-poly-L-**1**(+). Each single-handed helical living poly-L-**1** can be used as the macroinitiator for the enantiomer-selective and helix-sense-selective block copolymerizations of L-**1** and D-**1**, resulting in almost perfect single-handed helical block copolymers with different polymerization rate constants (k and k') regulated by the macromolecular helicity of the macroinitiators. (+) and (−) denote the Cotton effect signs of the polyisocyanides at 364 nm.

polymerization of racemic NCAs initiated by preformed α-helical D- or L-polypeptides.[6j−l] These pioneering studies are particularly interesting being relevant to the origin of the biomolecular homochirality.[7]

Recently, we reported the helix-sense-selective living polymerization of an optically active phenyl isocyanide bearing an L-alanine pendant with a long decyl chain (L-**1**) with the achiral μ-ethynediyl Pt−Pd catalyst (**2**)[8]that unprecedentedly produced both right (*P*)- and left (*M*)-handed helical, rigid-rod polyisocyanides (*P*-poly-L-**1**(+) and *M*-poly-L-**1**(−), respectively) at once with a different molecular weight (MW) and a narrow molecular weight distribution (MWD), which could be separated into each helix by facile fractionation with acetone.[9] The isolated single-handed helical polyisocyanides maintain their living feature and can be used as an initiator (macroinitiator) for further block copolymerizations of the isocyanides.[10] Taking full advantage of this unique characteristic of the living helical polyisocyanides with a controlled helical sense, the enantiomer-selective block copolymerizations of the L-**1** and D-**1** enantiomers were performed using the single-handed helical living poly-L-**1**'s with the opposite helical sense to each other as the macroinitiators (Figure 1). The results most clearly demonstrate a critical role of the chiral living growing chain end with a rigid single-handed helical conformation that contributes to a high enantiomer selectivity along with an almost perfect helix-sense selectivity during the block copolymerizations, thus providing further insight into the mechanism of chiral recognition by a growing end with a one-handed helical conformation.

(4) For reviews: (a) Pino, P. *Adv. Polym. Sci.* **1965**, *4*, 393–456. (b) Tsuruta, T. *J. Polym. Sci., Part D* **1972**, *6*, 179–250. (c) Okamoto, Y.; Yashima, E. *Prog. Polym. Sci.* **1990**, *15*, 263–298.

(5) For leading references of enantiomer-selective polymerizations of vinyl monomers: α-Olefins, (a) Pino, P.; Ciardelli, F.; Lorenzi, G. P.; Natta, G. *J. Am. Chem. Soc.* **1962**, *84*, 1487–1488. (b) Baar, C. R.; Levy, C. J.; Min, E. Y. J.; Henling, L. M.; Day, M. W.; Bercaw, J. E. *J. Am. Chem. Soc.* **2004**, *126*, 8216–8231. Methacrylates: (c) Okamoto, Y.; Ohta, K.; Yuki, H. *Chem. Lett.* **1977**, 617–620. (d) Okamoto, Y.; Urakawa, K.; Yuki, H. *J. Polym. Sci., Polym. Chem. Ed.* **1981**, *19*, 1385–1395. (e) Okamoto, Y.; Suzuki, K.; Kitayama, T.; Yuki, H.; Kageyama, H.; Miki, K.; Tanaka, N.; Kasai, N. *J. Am. Chem. Soc.* **1982**, *104*, 4618–4624. Divinyl derivatives, (f) Tsuji, M.; Sakai, R.; Satoh, T.; Kaga, H.; Kakuchi, T. *Macromolecules* **2002**, *35*, 8255–8257. (g) Narumi, A.; Sakai, R.; Ishido, S.; Sone, M.; Satoh, T.; Kaga, H.; Nakade, H.; Kakuchi, T. *Macromolecules* **2007**, *40*, 9272–9278.

(6) For leading references of enantiomer-selective polymerizations of cyclic monomers: Propylene oxide, (a) Inoue, S.; Tsuruta, T.; Furukawa, J. *Makromol. Chem.* **1962**, *53*, 215–218. (b) Tsuruta, T.; Inoue, S.; Yoshida, N.; Furukawa, J. *Makromol. Chem.* **1962**, *55*, 230–231. (c) Hirahata, W.; Thomas, R. M.; Lobkovsky, E. B.; Coates, G. W. *J. Am. Chem. Soc.* **2008**, *130*, 17658–17659. Propylene sulfide, (d) Furukawa, J.; Kawabata, N.; Kato, A. *J. Polym. Sci., Polym. Lett.* **1967**, *5*, 1073–1076. (e) Sépulchre, M.; Spassky, N.; Mark, C.; Schurig, V. *Makromol. Chem., Rapid Commun.* **1981**, *2*, 261–266. Aromatic thiiranes, (f) Imai, T.; Hayakawa, K.; Satoh, T.; Kaga, H.; Kakuchi, T. *J. Polym. Sci., Part A: Polym. Chem.* **2002**, *40*, 3443–3448. Lactones, (g) Spassky, N.; Leborgne, A.; Reix, M.; Prud'homme, R. E.; Bigdeli, E.; Lenz, R. W. *Macromolecules* **1978**, *11*, 716–719. (h) Le Borgne, A.; Spassky, N. *Polymer* **1989**, *30*, 2312–2319. Lactides, (i) Spassky, N.; Wisniewski, M.; Pluta, C.; Le Borgne, A. *Macromol. Chem. Phys.* **1996**, *197*, 2627–2637. α-Amino acid *N*-carboxy anhydrides (NCAs), (j) Doty, P.; Lundberg, R. D. *J. Am. Chem. Soc.* **1956**, *78*, 4810–4812. (k) Lundberg, R. D.; Doty, P. *J. Am. Chem. Soc.* **1957**, *79*, 3961–3972. (l) Matsuura, K.; Inoue, S.; Tsuruta, T. *Makromol. Chem.* **1964**, *80*, 149–157. (m) Hashimoto, Y.; Imanishi, Y. *Biopolymers* **1981**, *20*, 489–505. (n) Sendel, S. W.; Deming, T. J. *Macromolecules* **2003**, *36*, 969–972.

(7) (a) Feringa, B. L.; van Delden, R. A. *Angew. Chem., Int. Ed.* **1999**, *38*, 3418–3438. (b) Zepik, H.; Shavit, E.; Tang, M.; Jensen, T. R.; Kjaer, K.; Bolbach, G.; Leiserowitz, L.; Weissbuch, I.; Lahav, M. *Science* **2002**, *295*, 1266–1269. (c) Hans, R. K. *Angew. Chem., Int. Ed.* **2006**, *45*, 5752–5784.

(8) (a) Onitsuka, K.; Joh, T.; Takahashi, S. *Bull. Chem. Soc. Jpn.* **1992**, *65*, 1179–1181. (b) Onitsuka, K.; Joh, T.; Takahashi, S. *Angew. Chem., Int. Ed. Engl.* **1992**, *31*, 851–852.

(9) Onouchi, H.; Okoshi, K.; Kajitani, T.; Sakurai, S.-i.; Nagai, K.; Kumaki, J.; Onitsuka, K.; Yashima, E. *J. Am. Chem. Soc.* **2008**, *130*, 229–236.

(10) (a) Takei, F.; Yanai, K.; Onitsuka, K.; Takahashi, S. *Angew. Chem., Int. Ed. Engl.* **1996**, *35*, 1554–1556. (b) Takei, F.; Yanai, K.; Onitsuka, K.; Takahashi, S. *Chem.-Eur. J.* **2000**, *6*, 983–993. A similar helix-sense-selective cyclization polymerization of achiral 1,2-diisocyanobenzenes using a single-handed helical oligomer as an initiator was reported, see: (c) Ito, Y.; Ihara, E.; Murakami, M. *Angew. Chem., Int. Ed. Engl.* **1992**, *31*, 1509–1510. (d) Suginome, M.; Collet, S.; Ito, Y. *Org. Lett.* **2002**, *4*, 351–354.

Table 1. Block Copolymerization Results of L-**1**, D-**1**, and **Aib** Initiated by *M*-poly-L-$\mathbf{1}_{50}$(−), *M*-poly-L-$\mathbf{1}_{100}$(−), and *P*-poly-L-$\mathbf{1}_{100}$(+) in THF at 55 °C

run	polyisocyanide	time (h)	yield[a] (%)	SEC-UV[b] (PSt standard) $M_n \times 10^{-4}$	SEC-UV[b] M_w/M_n	SEC-MALS[c] $M_n \times 10^{-4}$	SEC-MALS[c] M_w/M_n	AFM observation L_n (nm)[d]	AFM observation L_w/L_n[d]	$[\alpha]^{25}_D$[e]	$\Delta\varepsilon_{364}$[e] (M^{-1} cm^{-1})	ee$_h$ (%)[f]	$k \times 10^5$ (s^{-1})[g]	k_L/k_D[h]
1	*M*-poly-L-$\mathbf{1}_{50}$(−)			10.3	1.03	3.08	1.03			−1782	−20.6			
2	*M*-poly-L-$\mathbf{1}_{50}$(−)-*b*-L-**1**	6	100	12.8	1.03	6.40	1.02			−1875	−22.1	∼100	9.18	7.65
3	*M*-poly-L-$\mathbf{1}_{50}$(−)-*b*-D-**1**	36	100	12.3	1.02	5.81	1.01			−1699	−20.3	99	1.20	
4	*M*-poly-L-$\mathbf{1}_{100}$(−)			12.4	1.08	5.97	1.05	15.0	1.05	−1847	−21.2			
5	*M*-poly-L-$\mathbf{1}_{100}$(−)-*b*-L-**1**	12	100	17.3	1.08	11.3	1.04	29.7	1.05	−1936	−22.6	∼100	5.99	6.37
6	*M*-poly-L-$\mathbf{1}_{100}$(−)-*b*-D-**1**	60	100	16.4	1.14	11.6	1.10	28.1	1.05	−1423	−19.3	91	0.94	
7	*M*-poly-L-$\mathbf{1}_{100}$(−)-*b*-**Aib**	30	100	18.0	1.08					−1903	−21.7	∼100	1.56	
8	*P*-poly-L-$\mathbf{1}_{100}$(+)			6.22	1.08	1.95	1.07			+1657	+20.2			
9	*P*-poly-L-$\mathbf{1}_{100}$(+)-*b*-L-**1**	30	100	9.79	1.04	3.60	1.03	7.95	1.05	+1767	+19.7	98	1.34	0.25(4.0)[i]
10	*P*-poly-L-$\mathbf{1}_{100}$(+)-*b*-D-**1**	10	100	8.79	1.06	3.86	1.02	8.82	1.07	+1901	+21.1	∼100	5.40	
11	*P*-poly-L-$\mathbf{1}_{100}$(+)-*b*-**Aib**	20	100	9.40	1.04					+1845	+20.4	∼100	2.04	

[a] Estimated by following the monomer conversions using SEC of the reaction mixture. [b] Determined by SEC (polystyrene standards) using UV−visible detector with THF containing TBAB (0.1 wt %) as the eluent. [c] Determined by SEC-MALS measurements with THF containing TBAB (0.1 wt %) as the eluent. [d] Estimated by AFM based on an evaluation of ca. 200 molecules. [e] Measured in $CHCl_3$ at 25 °C. [f] Helix-sense excess of block copolymers estimated on the basis of the $\Delta\varepsilon_{364}$ values of the corresponding macroinitiators. [g] Polymerization rate constants estimated by kinetic plots (see Figure 2B). [h] Enantiomer-selectivity ratio. [i] The k_D/k_L value is shown in parentheses.

Results and Discussion

Enantiomer-Selective Block Copolymerization. The single-handed helical poly-L-**1**'s were prepared by the living polymerization of L-**1** with achiral **2** as the catalyst in tetrahydrofuran (THF) at 55 °C ([L-**1**]/[**2**] = 100 for poly-L-$\mathbf{1}_{100}$ and [L-**1**]/[**2**] = 50 for poly-L-$\mathbf{1}_{50}$), followed by fractionation with acetone into the acetone-insoluble high MW *M*-poly-L-**1**(−) ($M_n = 6.0 \times 10^4$ for *M*-poly-L-$\mathbf{1}_{100}$(−) and $M_n = 3.0 \times 10^4$ for *M*-poly-L-$\mathbf{1}_{50}$(−)) and acetone-soluble low MW *P*-poly-L-**1**(+) ($M_n = 2.0 \times 10^4$ for *P*-poly-L-$\mathbf{1}_{100}$(+)) fractions, which showed negative and positive Cotton effect signs at 364 nm, respectively, according to a previously reported method (see Table 1).[9,11] The block copolymerizations of L-**1** and D-**1** using the *P*- and *M*-poly-L-**1**'s as the macroinitiators were conducted in THF at 55 °C in the presence of an internal polystyrene (PSt) standard. The copolymerization reactions were followed by measuring the size exclusion chromatography (SEC) in THF containing 0.1 wt % tetra-*n*-butylammonium bromide (TBAB) as the eluent using UV and circular dichroism (CD) detectors at appropriate time intervals to follow the changes in the relative MW of the copolymers with respect to PSt and to calculate the monomer conversions.

Figure 2A (a and b) shows the time-dependent SEC chromatograms for the block copolymerizations of L-**1** and D-**1** initiated by the left-handed helical *M*-poly-L-$\mathbf{1}_{100}$(−), respectively, which clearly revealed that the block copolymerizations proceeded in a living and enantiomer-selective manner, and L-**1** was preferentially copolymerized over the antipode D-**1**. The block copolymerizations of L-**1** and D-**1** were completed after 12 and 60 h, respectively, thus producing block copolymers (*M*-poly-L-$\mathbf{1}_{100}$(−)-*b*-L-**1** and *M*-poly-L-$\mathbf{1}_{100}$(−)-*b*-D-**1**, respectively) while maintaining narrow MWDs. The absolute number-average molecular weights (M_n) of the macroinitiator and the resulting block copolymers were determined by SEC coupled with multiangle light scattering (MALS) detector (SEC-MALS) measurements. The M_n values of the block copolymers are nearly twice as high as that of the macroinitiator (runs 4−6 in Table 1).

Both copolymerizations obey first-order kinetics. On the basis of the kinetic plots (a in Figure 2B), the copolymerization rate constants of L-**1** (k_L) and D-**1** (k_D) were estimated to be 5.99×10^{-5} and 9.4×10^{-6}, respectively, indicating that the reaction rate of L-**1** is approximately 6 times faster than that of D-**1** (Table 1). A lower MW macroinitiator with the same helical sense, *M*-poly-L-$\mathbf{1}_{50}$(−), also enantioselectively copolymerized L-**1** and D-**1** with the enantiomer-selectivity ratio (k_L/k_D) of 7.65 (runs 1−3 in Table 1, c in Figure 2B, and Figure S2). These results suggest a possible mechanism for the L-**1**-selective block copolymerization with the left-handed helical *M*-poly-L-**1**'s that may be controlled either by the chiral terminal L-**1** unit and/or by the left-handed helical conformation of the growing *M*-poly-L-**1** chains.

To provide a deeper insight into the enantiomer-selective mechanism, we employed the diastereomeric *P*-poly-L-$\mathbf{1}_{100}$(+) composed of the same L-**1** units, but possessing the opposite right-handed helical conformation in the main chain of that of the macroinitiator to copolymerize L-**1** and D-**1**. Quite interestingly, D-**1** was preferentially copolymerized over the L-**1** by a factor of 4.0 ($k_L/k_D = 0.25$), giving *P*-poly-L-$\mathbf{1}_{100}$(+)-*b*-D-**1** (runs 8−10 in Table 1, b in Figure 2B, and Figure S1). These results unambiguously proved the dominant role of the one-handed helical conformation of the growing chain that can efficiently discriminate the pair of enantiomers in a relatively high enantiomer selectivity, because D-**1** favorably homopolymerizes with **2** to give a right-handed helical *P*-poly-D-**1** as the major product.[9,12] The fact that the enantiomer selectivity of *P*-poly-L-$\mathbf{1}_{100}$(+) was slightly lower than that of the *M*-poly-L-$\mathbf{1}_{100}$(−) suggests that the chiral terminal L-**1** unit likely participates in the L-**1** enantiomer selection. The absolute M_n values of the block copolymers determined by SEC-MALS also nearly doubled when compared to that of the macroinitiator (runs 8−10 in Table 1).

Similar enantiomer-selective block copolymerization of an analogous phenyl isocyanide bearing an L- or D-menthyl residue as the pendant through an ester linkage using the helical polyisocyanides derived from the optically pure

(11) The helical sense (*P* or *M*) and helical sense excess (>97%) of the *M*-poly-L-**1**(−) and *P*-poly-L-**1**(+) were directly determined by high-resolution AFM observations.[9]

(12) A similar enantiomer-selective anionic polymerization of racemic phenyl-2-pyridyl-*o*-tolylmethyl methacrylate (PPyTMA) was performed using the preformed living poly(PPyTMA) with a one-handed helical conformation as the initiator, whose enantiomer selectivity was governed by the rigid helical structure of the growing polymer chain. See: (a) Yashima, E.; Okamoto, Y.; Hatada, K. *Macromolecules* **1988**, *21*, 854–855. See also: (b) Nakano, T.; Kinjo, N.; Hidaka, Y.; Okamoto, Y. *Polym. J.* **1999**, *31*, 464–469.

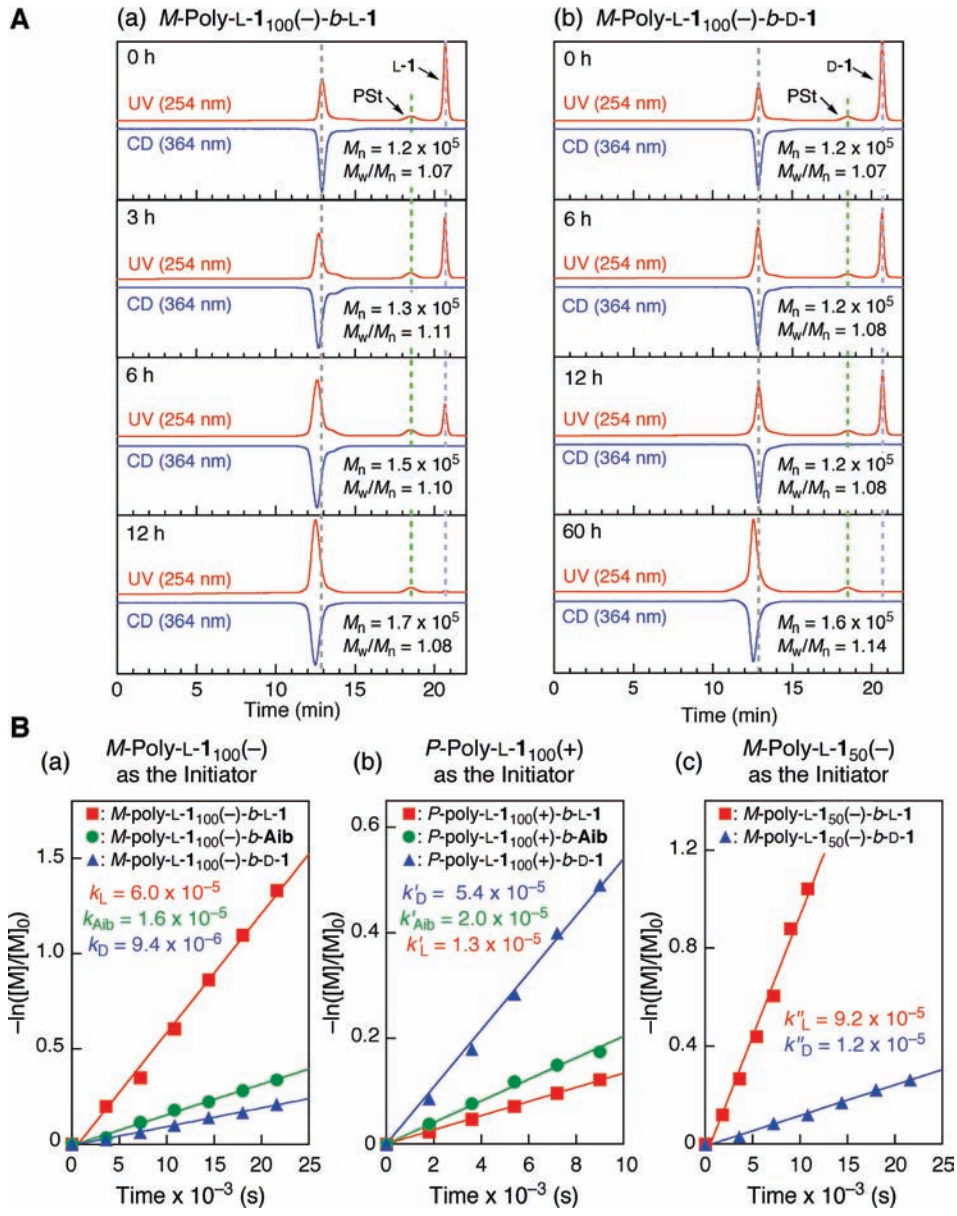

Figure 2. (A) SEC chromatograms for the block copolymerizations of L-**1** (a) and D-**1** (b) initiated by *M*-poly-L-$\mathbf{1}_{100}(-)$ in THF at 55 °C using UV (red lines) and CD (blue lines) detectors in THF containing 0.1 wt % TBAB as the eluent. The internal standard polystyrene (PSt) eluting at around 18.5 min was used to calculate the monomer conversions. The M_n and its distribution (M_w/M_n) of each polymer as determined by SEC (PSt standards) are also shown in (a) and (b). (B) First-order kinetic plots for the block copolymerizations of L-**1** (red ■) **Aib** (green ●), and D-**1** (blue ▲) initiated by *M*-poly-L-$\mathbf{1}_{100}(-)$ (a), *P*-poly-L-$\mathbf{1}_{100}(+)$ (b), and *M*-poly-L-$\mathbf{1}_{50}(-)$ (c) in THF at 55 °C. [macroinitiator] = 36 mg/mL, [**1** or **Aib**] = 36 mg/mL, [**1**]/[macroinitiator] = 167 (a), 54 (b), and 86 (c), and [**Aib**]/[macroinitiator] = 161 (a) and 52 (b).

isocyanide monomers as the macroinitiators was attempted.[10b] In sharp contrast to the present results, neither the enantiomer-selective nor helix-sense-selective polymerization took place during the block copolymerization, and the optical activity of the block copolymer composed of the L- and D-block segments significantly decreased. A one-handed helical conformation stabilized by intramolecular hydrogen bonds between the pendant amide residues of the helical poly-L-**1**'s, rather than steric interactions, appears to be indispensable for the simultaneous enantiomer-selective and helix-sense-selective block copolymerization as evidenced by the IR spectra of the resulting block copolymers in $CHCl_3$ (Figure S3).

As expected from the rigid rodlike features[13] of the resulting block copolymers as well as the macroinitiators with narrow MWDs, they exhibited smectic liquid crystalline phases as evidenced by their indisputably clear fan-shaped textures in concentrated $CHCl_3$ solutions under polarized optical micrographs (Figure 3).[9]

Helix-Sense-Selection during the Enantiomer-Selective Block Copolymerization. A number of helical polyisocyanides have been prepared by the polymerization of optically active isocyanides,[14] and one of the diastereomeric helices could be helix-sense selectively produced by the polymerization of an isocyanide enantiomer. As a consequence, the opposite helical polyisocyanide requires the polymerization of the opposite enantiomer, because the helix-sense of polyisocyanides is mostly

(13) Okoshi, K.; Nagai, K.; Kajitani, T.; Sakurai, S.-i.; Yashima, E. *Macromolecules* **2008**, *41*, 7752–7754.

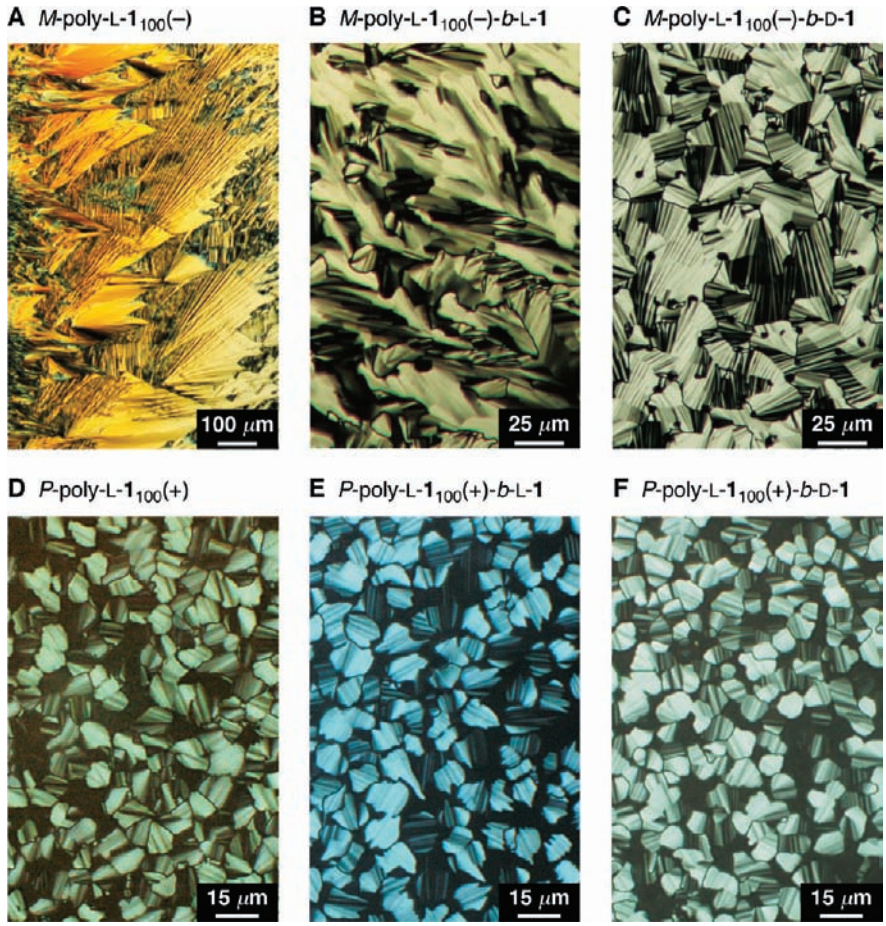

Figure 3. Polarized optical micrographs of the macroinitiators, *M*-poly-L-$\mathbf{1}_{100}(-)$ (A) and *P*-poly-L-$\mathbf{1}_{100}(+)$ (D), and the resulting block copolymers, *M*-poly-L-$\mathbf{1}_{100}(-)$-*b*-L-**1** (B), *M*-poly-L-$\mathbf{1}_{100}(-)$-*b*-D-**1** (C), *P*-poly-L-$\mathbf{1}_{100}(+)$-*b*-L-**1** (E), and *P*-poly-L-$\mathbf{1}_{100}(+)$-*b*-D-**1** (F), in $CHCl_3$ solution taken at ambient temperature. Clear fan-shaped textures typical of smectic phases were observed.

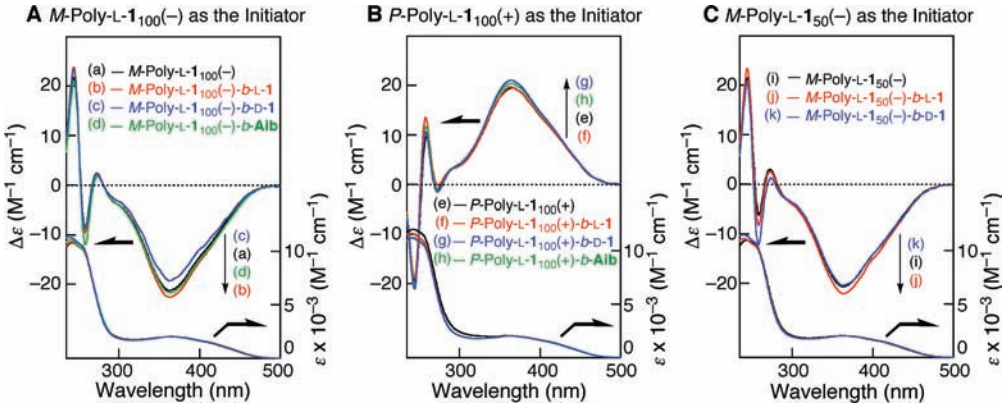

Figure 4. CD and absorption spectra of the macroinitiators and the resulting block copolymers measured in $CHCl_3$ at 25 °C (0.2 mg/mL). (A) Macroinitiator; *M*-poly-L-$\mathbf{1}_{100}(-)$ (a) and the block copolymers; *M*-poly-L-$\mathbf{1}_{100}(-)$-*b*-L-**1** (b), *M*-poly-L-$\mathbf{1}_{100}(-)$-*b*-D-**1** (c), and *M*-poly-L-$\mathbf{1}_{100}(-)$-*b*-**Aib** (d). (B) Macroinitiator; *P*-poly-L-$\mathbf{1}_{100}(+)$ (e) and the block copolymers; *P*-poly-L-$\mathbf{1}_{100}(+)$-*b*-L-**1** (f), *P*-poly-L-$\mathbf{1}_{100}(+)$-*b*-D-**1** (g), and *P*-poly-L-$\mathbf{1}_{100}(+)$-*b*-**Aib** (h). (C) Macroinitiator; *M*-poly-L-$\mathbf{1}_{50}(-)$ (i) and the block copolymers; *M*-poly-L-$\mathbf{1}_{50}(-)$-*b*-L-**1** (j) and *M*-poly-L-$\mathbf{1}_{50}(-)$-*b*-D-**1** (k).

biased by the molecular chirality of the monomer units.[15] This implies that the block copolymerization of D-**1**, for example, with *M*-poly-L-$\mathbf{1}_{100}(-)$ may produce a block copolymer consisting of the opposite helical block segments *M*-poly-L-$\mathbf{1}_{100}(-)$-*b*-*P*-poly-D-**1**(+), if the helix-sense of the polyisocyanide is determined by the chirality of the monomer units as already described. We then measured the CD and absorption spectra of the obtained macroinitiators and a series of block copolymers in $CHCl_3$ (Figure 4 and Table 1).[16]

Interestingly, the CD spectral patterns and intensities of the block copolyisocyanides in the imino chromophore regions of the polymer backbones (280−480 nm) as well as in the pendant aromatic regions (240−280 nm)[10b,17] are almost identical to those of the corresponding macroinitiators, although a slight

decrease in the CD intensities was observed for *M*-poly-L-$\mathbf{1}_{100}(-)$-*b*-D-**1** (run 6 in Table 1) and *P*-poly-L-$\mathbf{1}_{100}(+)$-*b*-L-**1** (run 9). These results clearly demonstrate that the present living block copolymerizations proceed in an extremely high helix-sense-selective fashion together with a high enantiomer selectivity, and the preformed helical handedness of the macroinitiators determines the overall helical sense of the block polyisocyanides irrespective of the configuration of the isocyanide monomers during the block copolymerizations, which may be mostly kinetically governed, rather than thermodynamically.[18]

Taking advantage of the high helix-sense selectivity of the *M*- and *P*-poly-L-**1**'s while maintaining the polymerization activity,[19] an analogous achiral isocyanide, 4-isocyanobenzoyl-2-aminoisobutyric acid decyl ester (**Aib**), was found to be helix-sense-selectively copolymerized with *M*-poly-L-$\mathbf{1}_{100}(-)$ and *P*-poly-L-$\mathbf{1}_{100}(+)$ (Figures 2B), resulting in the block copolymers with narrow MWDs. The block copolymers, *M*-poly-L-$\mathbf{1}_{100}(-)$-*b*-**Aib** and *P*-poly-L-$\mathbf{1}_{100}(+)$-*b*-**Aib**, also exhibited as intense CDs as those of the *M*-poly-L-$\mathbf{1}_{100}(-)$-*b*-L-**1** and *P*-poly-L-$\mathbf{1}_{100}(+)$-*b*-D-**1** (runs 7 and 11 in Table 1 and Figure 4).[10a,b]

AFM Observations of Molecular Length and Helical-Sense of Block Copolymers. Previously, we developed a facile method to directly observe the helical structures of certain helical polymers[9,20] including the *P*- and *M*-poly-L-**1**'s at a molecular resolution by AFM.[9,15a] The rodlike helical poly-L-**1**'s hierarchically self-assembled into smectic-like two-dimensional (2D) helix-bundles on highly oriented pyrolytic graphite (HOPG) upon exposure to benzene or THF vapors. The high-resolution AFM images of the poly-L-**1**'s on HOPG enabled us to determine their molecular length, helical pitch, and handedness.

Given the success in visualizing the helical structures of the poly-L-**1**'s by AFM, we applied this procedure to visually reveal the present living and helix-sense-selective block copolymerizations by measuring the high-resolution AFM images of block copolymers of *M*-poly-L-$\mathbf{1}_{100}(-)$ and *P*-poly-L-$\mathbf{1}_{100}(+)$ with L-**1** and D-**1**. Figure 5 shows the typical AFM images of the macroinitiator, *M*-poly-L-$\mathbf{1}_{100}(-)$, and its block copolymers, *M*-poly-L-$\mathbf{1}_{100}(-)$-*b*-L-**1** and *M*-poly-L-$\mathbf{1}_{100}(-)$-*b*-D-**1**, deposited on HOPG from a dilute THF solution after THF vapor exposure at ambient temperature for 2 h. The 2D smectic-like layer structures composed of self-assembled polymer chains were observed. The number-average molecular length (L_n) of the individual polymer chains increased with the increasing M_n of the polyisocyanides, 15.0, 29.7, and 28.1 nm for *M*-poly-L-$\mathbf{1}_{100}(-)$, *M*-poly-L-$\mathbf{1}_{100}(-)$-*b*-L-**1**, and *M*-poly-L-$\mathbf{1}_{100}(-)$-*b*-D-**1**, respectively. A similar tendency was also observed for the block copolymers initiated by the *P*-poly-L-$\mathbf{1}_{100}(+)$ (see Figure S5). Thus, the L_n values of the block copolymers nearly doubled in length as compared to those of the macroinitiators as supported by the SEC-MALS measurement results (Table 1 and see also Figure S4).

As well as the molecular lengths, the helical senses of the macroinitiator, *M*-poly-L-$\mathbf{1}_{100}(-)$,[9] and its block copolymers, *M*-poly-L-$\mathbf{1}_{100}(-)$-*b*-L-**1** and *M*-poly-L-$\mathbf{1}_{100}(-)$-*b*-D-**1**, could also be directly determined by high-resolution AFM (Figure 6A and B, respectively), in which the left-handed helical structures with a helical pitch of about 1.3−1.4 nm are predominantly ob-

(14) For reviews on helical polyisocyanides, see refs 1b and 1h, and: (a) Millich, F. *Chem. Rev.* **1972**, *72*, 101–113. (b) Millich, F. *Adv. Polym. Sci.* **1975**, *19*, 117–141. (c) Drenth, W.; Nolte, R. J. M. *Acc. Chem. Res.* **1979**, *12*, 30–35. (d) Takahashi, S.; Onitsuka, K.; Takei, F. *Proc. Jpn. Acad., Ser. B* **1998**, *74*, 25–30. (e) Suginome, M.; Ito, Y. *Adv. Polym. Sci.* **2004**, *171*, 77–136. (f) Amabilino, D. B.; Serrano, J.-L.; Sierra, T.; Veciana, J. *J. Polym. Sci., Part A: Polym. Chem.* **2006**, *44*, 3161–3174. For other leading references of helical polyisocyanides, see: (g) Kamer, P. C. J.; Nolte, R. J. M.; Drenth, W. *J. Am. Chem. Soc.* **1988**, *110*, 6818–6825. (h) Green, M. M.; Gross, R. A.; Schilling, F. C.; Zero, K.; Crosby, C. I. *Macromolecules* **1988**, *21*, 1839–1846. (i) Pini, D.; Iuliano, A.; Salvadori, P. *Macromolecules* **1992**, *25*, 6059–6062. (j) Spencer, L.; Kim, M.; Euler, W. B.; Rosen, W. *J. Am. Chem. Soc.* **1997**, *119*, 8129–8130. (k) Cornelissen, J. J. L. M.; Fischer, M.; Sommerdijk, N. A. J. M.; Nolte, R. J. M. *Science* **1998**, *280*, 1427–1430. (l) Amabilino, D. B.; Ramos, E.; Serrano, J.-L.; Veciana, J. *Adv. Mater.* **1998**, *10*, 1001–1005. (m) Amabilino, D. B.; Ramos, E.; Serrano, J.-L.; Sierra, T.; Veciana, J. *J. Am. Chem. Soc.* **1998**, *120*, 9126–9134. (n) Hasegawa, T.; Kondoh, S.; Matsuura, K.; Kobayashi, K. *Macromolecules* **1999**, *32*, 6595–6603. (o) Cornelissen, J. J. L. M.; Donners, J. J. J. M.; de Gelder, R.; Graswinckel, W. S.; Metselaar, G. A.; Rowan, A. E.; Sommerdijk, N. A. J. M.; Nolte, R. J. M. *Science* **2001**, *293*, 676–680. (p) Yamada, Y.; Kawai, T.; Abe, J.; Iyoda, T. *J. Polym. Sci., Part A: Polym. Chem.* **2002**, *40*, 399–408. (q) Cornelissen, J. J. L. M.; Graswinckel, W. S.; Rowan, A. E.; Sommerdijk, N. A. J. M.; Nolte, R. J. M. *J. Polym Sci., Part A: Polym. Chem.* **2003**, *41*, 1725–1736. (r) Amabilino, D. B.; Ramos, E.; Serrano, J.-L.; Sierra, T.; Veciana, J. *Polymer* **2005**, *46*, 1507–1521. (s) Onitsuka, K.; Mori, T.; Yamamoto, M.; Takei, F.; Takahashi, S. *Macromolecules* **2006**, *39*, 7224–7231.

(15) We recently reported the unprecedented helix-sense controlled polymerization of L-**1**. The polymerization of L-**1** with an achiral nickel catalyst diastereoselectively proceeded, resulting in either right- or left-handed helical poly-L-**1**, whose helix-sense was controlled by the polymerization solvent and temperature: (a) Kajitani, T.; Okoshi, K.; Sakurai, S.-i.; Kumaki, J.; Yashima, E. *J. Am. Chem. Soc.* **2006**, *128*, 708–709. (b) Kajitani, T.; Okoshi, K.; Yashima, E. *Macromolecules* **2008**, *41*, 1601–1611, Similar diastereomeric helical polyisocyanides were also prepared by the copolymerization between achiral and chiral isocyanides or two different chiral isocyanides based on the selective growth inhibition of a one screw-sense. See refs 14g and 14l.

(16) The CD spectral patterns and intensities of polyisocyanides measured in $CHCl_3$ (Figure 4A) were almost identical to those in THF.

(17) (a) Takei, F.; Hayashi, H.; Onitsuka, K.; Kobayashi, N.; Takahashi, S. *Angew. Chem., Int. Ed.* **2001**, *40*, 4092–4094. (b) Ishikawa, M.; Maeda, K.; Mitsutsuji, Y.; Yashima, E. *J. Am. Chem. Soc.* **2004**, *126*, 732–733. (c) Hase, Y.; Mitsutsuji, Y.; Ishikawa, M.; Maeda, K.; Okoshi, K.; Yashima, E. *Chem. Asian J.* **2007**, *2*, 755–763. (d) Miyabe, T.; Hase, Y.; Iida, H.; Maeda, K.; Yashima, E. *Chirality* **2009**, *21*, 44–50.

(18) For helix-sense-selective polymerization of achiral bulky isocyanides with chiral initiators or catalysts, see refs 1b, 1h, 14e, and 14g, and: (a) Deming, T. J.; Novak, B. M. *J. Am. Chem. Soc.* **1992**, *114*, 7926–7927. For helix-sense-selective block copolymerization of achiral isocyanides or chiral isocyanides using optically active polyisocyanide prepolymers as initiators, see refs 10a−c. For helix-sense-selective and enantiomer-selective block copolymerization of chiral isocyanides using optically active polyisocyanide prepolymers as initiators, see: (b) Metselaar, G. A.; Cornelissen, J. J. L. M.; Rowan, A. E.; Nolte, R. J. M. *Angew. Chem., Int. Ed.* **2005**, *44*, 1990–1993. For leading references of helix-sense-selective polymerization of other achiral monomers using chiral initiators or catalysts: Methacrylates,[1a,g,4c] (c) Okamoto, Y.; Suzuki, K.; Ohta, K.; Hatada, K.; Yuki, H. *J. Am. Chem. Soc.* **1979**, *101*, 4763–4765. (d) Nakano, T.; Okamoto, Y.; Hatada, K. *J. Am. Chem. Soc.* **1992**, *114*, 1318–1329. Methacrylamides, (e) Hoshikawa, N.; Hotta, Y.; Okamoto, Y. *J. Am. Chem. Soc.* **2003**, *125*, 12380–12381. (f) Miyake, G. M.; Mariott, W. R.; Chen, E. Y.-X. *J. Am. Chem. Soc.* **2007**, *129*, 6724–6725. Cholorals, (g) Corley, L. S.; Vogl, O. *Polym. Bull.* **1980**, *3*, 211–217. (h) Vogl, O.; Jaycox, G. D.; Kratky, C.; Simonsick, W. J.; Hatada, K. *Acc. Chem. Res.* **1992**, *25*, 408–413. Isocyanates, (i) Okamoto, Y.; Matsuda, M.; Nakano, T.; Yashima, E. *Polym. J.* **1993**, *25*, 391–396. (j) Maeda, K.; Okamoto, Y. *Polym. J.* **1998**, *30*, 100–105. Acetylenes, (k) Aoki, T.; Kaneko, T.; Maruyama, N.; Sumi, A.; Takahashi, M.; Sato, T.; Teraguchi, M. *J. Am. Chem. Soc.* **2003**, *125*, 6346–6347. Carbodiimides, (l) Tian, G.; Lu, Y.; Novak, B. M. *J. Am. Chem. Soc.* **2004**, *126*, 4082–4083. (m) Tang, H.-Z.; Boyle, P. D.; Novak, B. M. *J. Am. Chem. Soc.* **2005**, *127*, 2136–2142.

(19) The living polyisocyanides prepared by the μ-ethynediyl Pt-Pd catalyst (**2**) are thermally stable in solution at 55 °C for 24 h and in the solid state at least for a year and maintain its polymerization activity.

(20) (a) Sakurai, S.-i.; Okoshi, K.; Kumaki, J.; Yashima, E. *Angew. Chem., Int. Ed.* **2006**, *45*, 1245–1248. (b) Sakurai, S.-i.; Okoshi, K.; Kumaki, J.; Yashima, E. *J. Am. Chem. Soc.* **2006**, *128*, 5650–5651. (c) Sakurai, S.-i.; Ohsawa, S.; Nagai, K.; Okoshi, K.; Kumaki, J.; Yashima, E. *Angew. Chem., Int. Ed.* **2007**, *46*, 7605–7608.

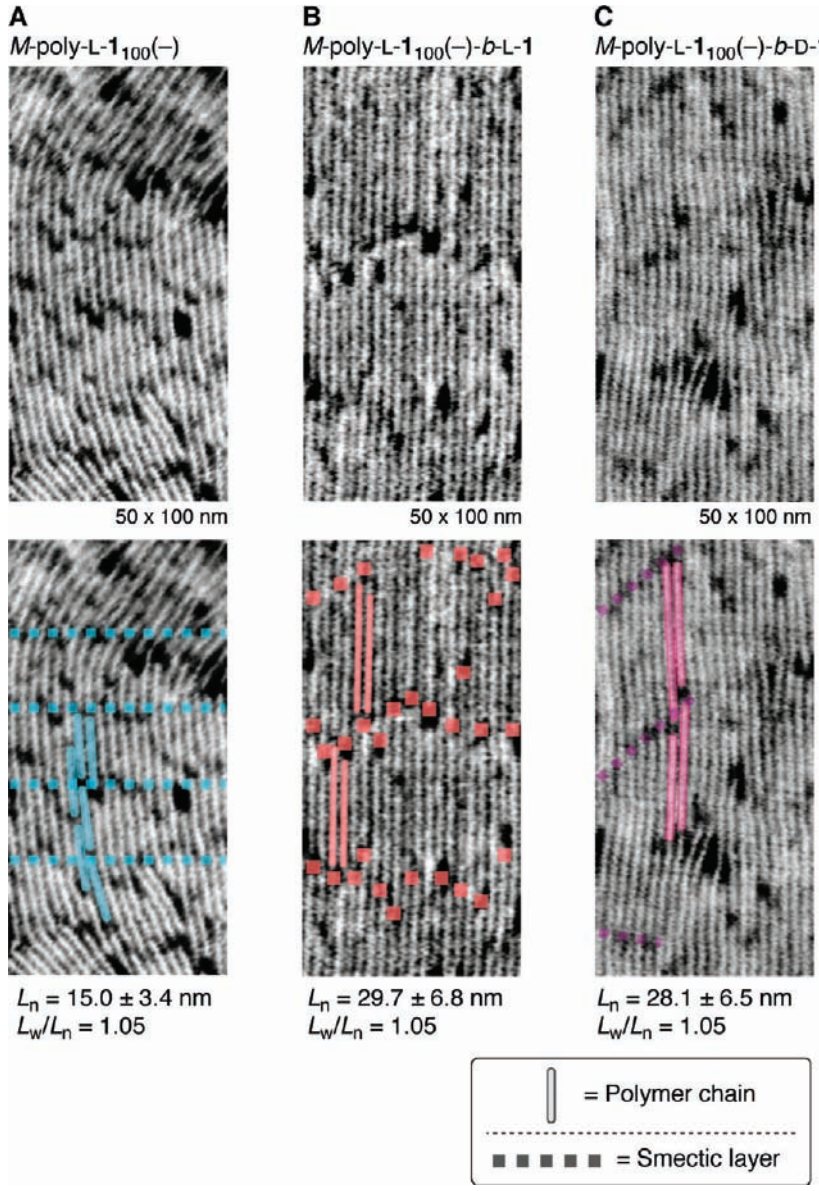

Figure 5. AFM phase images of 2D self-assembled *M*-poly-L-$\mathbf{1}_{100}(-)$ (A), *M*-poly-L-$\mathbf{1}_{100}(-)$-*b*-L-**1** (B), and *M*-poly-L-$\mathbf{1}_{100}(-)$-*b*-D-**1** (C) on HOPG (top). Scale = 50 × 100 nm. The bars and dotted lines in the images (bottom) indicate the individual polymer chains and 2D smectic layers, respectively.

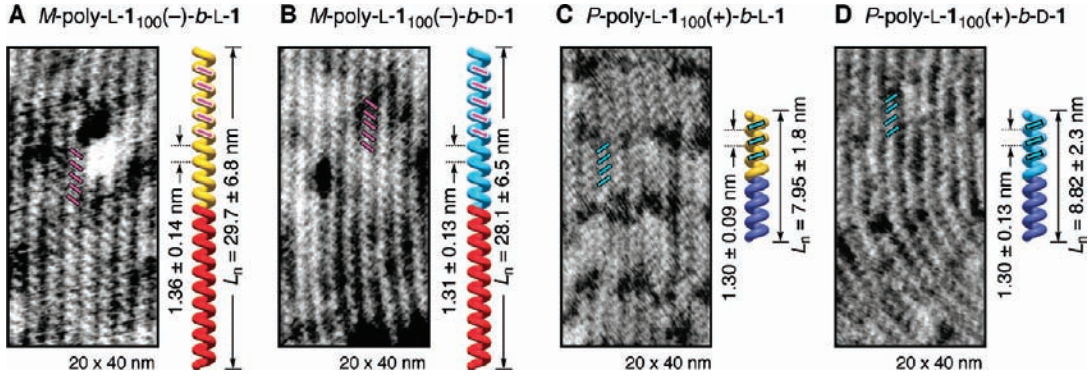

Figure 6. AFM phase images of 2D self-assembled block copolymers, *M*-poly-L-$\mathbf{1}_{100}(-)$-*b*-L-**1** (A), *M*-poly-L-$\mathbf{1}_{100}(-)$-*b*-D-**1** (B), *P*-poly-L-$\mathbf{1}_{100}(+)$-*b*-L-**1** (C), and *P*-poly-L-$\mathbf{1}_{100}(+)$-*b*-D-**1** (D), on HOPG (scale 20 × 40 nm). Schematic representations of the left-handed helical *M*-poly-L-$\mathbf{1}_{100}(-)$-*b*-L-**1** and *M*-poly-L-$\mathbf{1}_{100}(-)$-*b*-D-**1** and right-handed helical *P*-poly-L-$\mathbf{1}_{100}(+)$-*b*-L-**1** and *P*-poly-L-$\mathbf{1}_{100}(+)$-*b*-D-**1** with periodic oblique stripes (pink and blue lines, respectively), which denote a one-handed helical array of the pendants, are also shown (right). The number-average molecular length (L_n) and the length distribution (L_w/L_n) were also estimated on the basis of an evaluation of ca. 200 molecules (see also Table 1).

served.[21] In contrast to the *M*-poly-L-$\mathbf{1}_{100}(-)$ and its block copolymers, the right-handed helical structures with a helical pitch of about 1.3 nm are observed for *P*-poly-L-$\mathbf{1}_{100}(+)$[9] and its block copolymers, *P*-poly-L-$\mathbf{1}_{100}(+)$-*b*-L-**1** and *P*-poly-L-$\mathbf{1}_{100}(+)$-*b*-D-**1** (Figure 6C and D, respectively). Consequently, these remarkable high-resolution AFM images visually support the almost perfect helix-sense-selectivity during the living block copolymerizations of L-**1** and D-**1** with *M*-poly-L-$\mathbf{1}_{100}(-)$ and *P*-poly-L-$\mathbf{1}_{100}(+)$ as the macroinitiators.

Conclusions

In summary, we have demonstrated that the living block copolymerizations of isocyanide enantiomers initiated by rigid-rod helical polyisocyanides composed of either a right- or a left-handed helical growing chain proceeded in a high enantiomer-selective manner with an unprecedentedly high helix-sense selectivity, resulting in almost perfect one-handed helical block polyisocyanides whose helical senses are totally regulated by the helical chirality of the living polyisocyanide chains used as the initiators irrespective of the configuration of the monomer units of the living polyisocyanides during the block copolymerizations. The present unique enantiomer- and helix-sense-selective living block copolymerizations are for the first time unambiguously proven by direct observations of the molecular lengths and helical structures of the polyisocyanides before and after the block copolymerizations by high-resolution AFM.

We believe that the present methodology will be useful for developing novel smectic liquid crystalline, rigid-rod block polyisocyanides composed of different and desired monomer units with a controlled helicity through the living block copolymerization that may also provide unique chiral materials for separating enantiomers and asymmetric catalysts derived from controlled helical architectures.

Experimental Section

Instruments. The NMR spectra were measured using a Varian AS500 spectrometer (Varian, Palo Alto, CA) operating at 500 MHz for ^{1}H and 125 MHz for ^{13}C using TMS as the internal standard. The IR spectra were recorded using a JASCO FT/IR-680 spectrometer (JASCO, Tokyo, Japan). The absorption and CD spectra were obtained in a 1.0 mm quartz cell at 25 °C using a JASCO V570 spectrophotometer and a JASCO J820 spectropolarimeter, respectively. The polymer concentration was calculated on the basis of the monomer units and was 0.2 mg/mL. The optical rotations were measured in a 2 cm quartz cell on a JASCO P-1030 polarimeter. SEC was performed using a JASCO PU-2080 liquid chromatograph equipped with UV−visible (JASCO UV-2070) and CD (JASCO CD-2095) detectors. Two Tosoh TSKgel Multipore-H_{XL}-M SEC columns (Tosoh, Tokyo, Japan) were connected in series, and THF containing 0.1 wt % tetra-*n*-butylammonium bromide (TBAB) was used as the eluent at the flow rate of 1.0 mL/min. The molecular weight calibration curve was obtained with standard polystyrenes (Tosoh). The SEC-MALS measurements were performed using an HLC-8220 GPC system (Tosoh) equipped with a differential refractometer coupled to a DAWN-EOS MALS device equipped with a semiconductor laser (λ = 690 nm) (Wyatt Technology, Santa Barbara, CA) operated at 25 °C using two TSKgel Multipore H_{XL}-M columns (Tosoh) in series. The scattered light intensities were measured by 18 light scattering detectors at different angles. The differential refractive index increment, d*n*/d*c*, of the polymer with respect to the mobile phase at 25 °C was also measured by an Optilab rEX interferometric refractometer (Wyatt Technology). The AFM measurements were performed using a Nanoscope IIIa or Nanoscope IV microscope (Veeco Instruments, Santa Barbara, CA) in air at ambient temperature (ca. 25 °C) with standard silicon cantilevers (NCH, NanoWorld, Neuchâtel, Switzerland) in the tapping mode.

Scheme 1. Synthesis of **Aib**

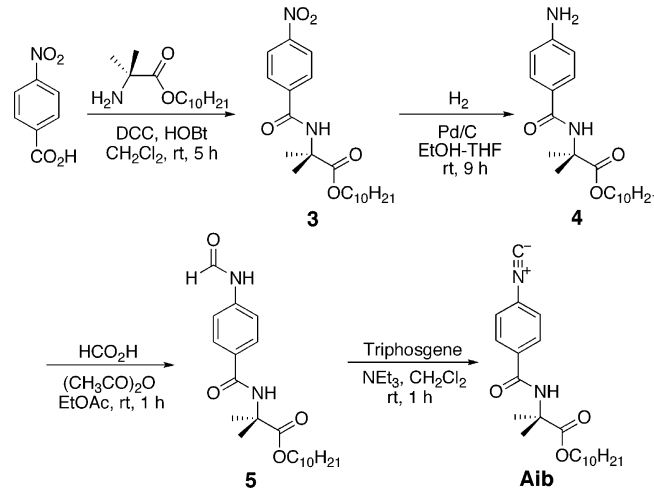

Materials. Anhydrous THF, CH_2Cl_2, $CHCl_3$, ethyl acetate, and ethanol (water content < 50 ppm) were purchased from Wako (Osaka, Japan) and stored under dry nitrogen. THF was further dried over sodium benzophenone ketyl, distilled onto $LiAlH_4$ under nitrogen, and distilled under high vacuum just before use. Palladium 10% activated carbon, 4-nitrobenzoic acid, *N*,*N*′-dicyclohexylcarbodiimide (DCC), 1-hydroxybenzotriazole monohydrate (HOBt), formic acid, acetic anhydride, triphosgene, and triethylamine were purchased from Wako, Tokyo Kasei (TCI, Tokyo, Japan), or Aldrich. These reagents were used without further purification. The 4-isocyanobenzoyl-L- and D-alanine decyl esters (L-**1** and D-**1**)[15a] and the μ-ethynediyl Pt−Pd complex (**2**)[8a] were prepared as previously reported. 4-Isocyanobenzoyl-2-aminoisobutyric acid decyl ester (**Aib**) was prepared according to Scheme 1.

Synthesis of 3. HOBt (4.58 g, 29.9 mmol) and DCC (6.17 g, 29.9 mmol) were added to a solution of 4-nitrobenzoic acid (5.00 g, 29.9 mmol) in dry CH_2Cl_2 (100 mL). After the reaction mixture was stirred at 0 °C for 30 min under Ar, the 2-aminoisobutyric acid decyl ester (7.26 g, 29.9 mmol), which had been prepared from 2-aminoisobutyric acid and 1-decanol by the conventional method,[22] was added to the mixture. The dispersion solution was stirred at room temperature for 5 h. After filtration, the solvent was removed by evaporation. The crude product was purified by silica gel chromatography with $CHCl_3$ as the eluent and then recrystallized with hexane−ethyl acetate (1:2, v/v) to give **3** as a white crystalline solid (7.03 g, 60%). Mp 67.6−68.5 °C. IR (KBr, cm^{-1}): 3308 (ν_{N-H}), 1739 ($\nu_{C=O}$ ester), 1649 (amide I), 1528 (amide II). ^{1}H NMR ($CDCl_3$, rt, 500 MHz): δ 0.88 (t, J = 6.8 Hz, CH_3, 3H), 1.26−1.35 (m, CH_2, 14H), 1.65−1.70 (m, CH_2, 2H), 1.75 (s, CH_3, 6H), 4.18−4.21 (m, CH_2, 2H), 7.08 (br, NH, 1H), 7.97 (d, J = 8.0 Hz aromatic, 2H), 8.29 (d, J = 8.0 Hz, aromatic, 2H). ^{13}C NMR ($CDCl_3$, rt, 125 MHz): δ 14.33, 18.81, 22.88, 26.03, 28.73, 29.42, 29.50, 29.72, 29.72, 32.09, 49.09, 66.31, 124.07, 128.49, 139.82, 150.01, 164.93, 173.21.

Synthesis of 4. Palladium-activated carbon (0.80 g) was added to a solution of **3** (3.11 g, 7.93 mmol) in ethanol (20 mL) and THF (20 mL). The mixture was stirred at room temperature for 9 h under an atmosphere of H_2. After filtration using Celite, the solvent was removed by evaporation. The crude product was then purified by

(21) The AFM images of larger areas (Figure S6) revealed that the left-handed helical *M*-poly-L-$\mathbf{1}_{100}(-)$-*b*-D-**1** (d in Figure S6) is composed of very few opposite right-handed helical segments, which agreed with a slight decrease in its CD intensity (Table 1).

(22) Okoshi, K.; Sakajiri, K.; Kumaki, J.; Yashima, E. *Macromolecules* **2005**, *38*, 4061–4064.

Scheme 2. Synthesis of Living Macroinitiators *M*-poly-L-**1**$_{50}$(−), *M*-poly-L-**1**$_{100}$(−), and *P*-poly-L-**1**$_{100}$(+)

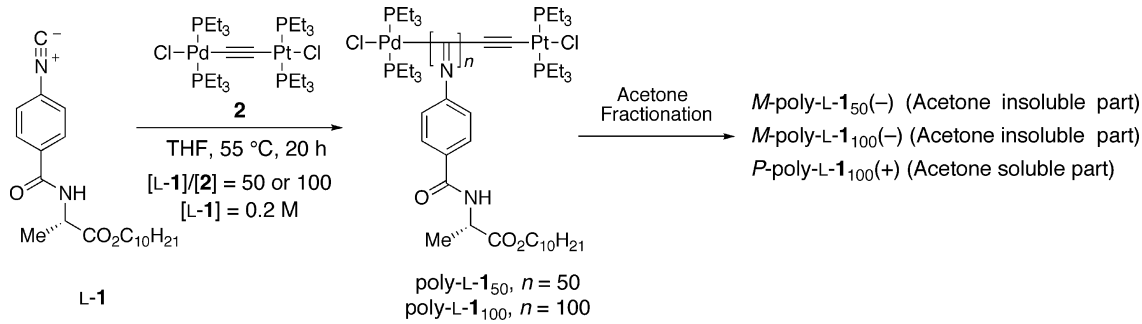

recrystallization with hexane−ethyl acetate (1:3, v/v) to give **4** as a white crystalline solid (2.61 g, 91%). Mp 78.6−79.5 °C. IR (KBr, cm^{-1}): 3448 (ν_{N-H}), 3334 (ν_{N-H}), 1727 ($\nu_{C=O}$ ester), 1628 (amide I), 1535 (amide II). ^{1}H NMR ($CDCl_3$, rt, 500 MHz): δ 0.85 (t, J = 6.5 Hz, CH_3, 3H), 1.26−1.36 (m, CH_2, 14H), 1.56−1.64 (m, CH_2, 2H), 1.70 (s, CH_3, 6H), 3.97 (s, NH_2, 2H), 4.16−4.21 (m, CH_2, 2H), 6.56 (d, J = 7.0 Hz, NH, 1H), 6.69 (d, J = 8.5 Hz, aromatic, 2H), 7.64 (d, J = 8.5 Hz, aromatic, 2H). ^{13}C NMR ($CDCl_3$, rt, 125 MHz): δ 13.92, 22.48, 24.71, 26.04, 28.76, 29.42, 29.51, 29.71, 29.73, 32.10, 58.64, 66.41, 113.81, 123.41, 128.54, 149.86, 166.04, 175.87.

Synthesis of 5. After a mixture of formic acid (1.08 mL, 28.7 mmol) and acetic anhydride (0.543 mL, 5.74 mmol) was stirred at room temperature for 1 h under Ar, **4** (2.08 g, 5.74 mmol) in dry ethyl acetate (50 mL) was added to the mixture at 0 °C. The dispersion solution was stirred at 0 °C for 30 min, and then at room temperature for 30 min. To the solution was added ethyl acetate (50 mL), and the mixture was filtered. The filtrate was washed with H_2O (100 mL) and brine (100 mL) and then dried over anhydrous $MgSO_4$. After the solvent was removed by evaporation, the crude product was purified by SEC with $CHCl_3$ as the eluent and then recrystallized with hexane−ethyl acetate (1:3, v/v) to give **5** as a white crystalline solid (2.15 g, 96%). Mp 151.1−151.8 °C. IR (KBr, cm^{-1}): 3343 (ν_{N-H}), 3290 (ν_{N-H}), 1733 ($\nu_{C=O}$ ester), 1634 (amide I), 1536 (amide II). ^{1}H NMR ($CDCl_3$, rt, 500 MHz): δ 0.89 (t, J = 6.8 Hz, CH_3, 3H), 1.26−1.36 (m, CH_2, 14H), 1.63−1.69 (m, CH_2, 2H), 1.73 (s, CH_3, 6H), 4.12−4.22 (m, CH_2, 2H), 6.93 (d, J = 7.0 Hz, NH in *trans*, 0.35H), 6.97 (d, J = 7.0 Hz, NH in *cis*, 0.65H), 7.12 (d, J = 8.5 Hz, H_o to NH in *trans*, 0.7H), 7.61 (d, J = 8.5 Hz, H_o to NH in *cis*, 1.3H), 7.75 (d, J = 8.5 Hz, H_m to NH in *cis*, 1.3H), 7.79 (d, J = 8.5 Hz, H_m to NH in *trans*, 0.7H), 8.37 (s, HCO in *cis*, 0.65H), 8.42 (d, J = 4.5 Hz, NH in *cis*, 0.65H), 8.63 (d, J = 11.0 Hz, HCO in *trans*, 0.35H), 8.79 (d, J = 11.0 Hz, NH in *trans*, 0.35H). The *cis* and *trans* conformers are tentatively assigned based on the literature.[14m] ^{13}C NMR ($CDCl_3$, rt, 125 MHz): δ 14.32, 22.88, 25.01, 26.02, 28.74, 29.41, 29.50, 29.70, 29.72, 32.09, 57.47, 66.09, 117.81, 119.66, 130.43, 131.15, 139.31, 140.60, 159.65, 161.99, 166.17, 166.62, 175.71.

Synthesis of Aib. Triethylamine (0.148 mL, 1.06 mmol) was added to a solution of **5** (207 mg, 0.531 mmol) in dry CH_2Cl_2 (6 mL). After the reaction mixture was stirred at 0 °C for 10 min under Ar, a solution of triphosgene (87.0 mg, 0.292 mmol) in CH_2Cl_2 (10 mL) was added dropwise to the mixture using a syringe. The dispersion solution was stirred at room temperature for 1 h, and then CH_2Cl_2 (50 mL) was added. After filtration, the solution was washed with aqueous $NaHCO_3$ (100 mL) and dried over anhydrous $MgSO_4$. The solvent was removed by evaporation, and the crude product was purified by silica gel chromatography with $CHCl_3$ as the eluent and then recrystallized with hexane−ethyl acetate (1:1, v/v) to give **Aib** as a white crystalline solid (162 mg, 82%). Mp 67.6−68.5 °C. IR (KBr, cm^{-1}): 3303 (ν_{N-H}), 2119 ($\nu_{C\equiv N}$), 1736 ($\nu_{C=O}$ ester), 1645 (amide I), 1535 (amide II). ^{1}H NMR ($CDCl_3$, rt, 500 MHz): δ 0.88 (t, J = 7.0 Hz, CH_3, 3H), 1.25−1.32 (m, CH_2, 14H), 1.64−1.69 (m, CH_2, 2H), 1.70 (s, CH_3, 6H), 4.17−4.20 (m, CH_2, 2H), 6.92 (d, J = 6.5 Hz, NH, 1H), 7.45 (d, J = 8.5 Hz, aromatic, 2H), 7.82 (d, J = 8.5 Hz, aromatic, 2H). ^{13}C NMR ($CDCl_3$, rt, 125 MHz): δ 14.32, 22.89, 24.44, 26.01, 28.74, 29.39, 29.50, 29.70, 29.73, 32.09, 57.00, 66.24, 126.89, 128.60, 135.06, 159.45, 164.99, 167.03, 175.34. Anal. Calcd for $C_{22}H_{32}N_2O_3$ (372.2): C, 70.94; H, 8.66; N, 7.52. Found: C, 71.17; H, 8.63; N, 7.56.

Preparation of Single-Handed Helical Poly(phenyl isocyanide) Macroinitiators. The single-handed helical poly(phenyl isocyanide) macroinitiators were prepared as outlined in Scheme 2 in a way similar to that previously reported.[9] The polymerization of L-**1** was carried out in a dry glass ampule under a dry nitrogen atmosphere using **2** as the catalyst to obtain poly-L-**1**. The poly-L-**1** was then fractionated into left-handed helical *M*-poly-L-**1**(−) and right-handed helical *P*-poly-L-**1**(+) using acetone. The resulting *M*-poly-L-**1**(−) and *P*-poly-L-**1**(+) were used as the macroinitiators.

A typical experimental procedure is described below. Monomer L-**1** (300 mg, 0.84 mmol) was placed in a dry ampule, which was then evacuated on a vacuum line and flushed with dry nitrogen. After this evacuation-flush procedure had been repeated three times, a three-way stopcock was attached to the ampule, and dry THF (3.4 mL) was added by a syringe. To this was added a solution of **2** in THF (10 μM, 0.81 mL) at ambient temperature. The concentrations of L-**1** and **2** were 0.2 and 0.002 M, respectively ([**1**]/[**2**] = 100). The mixture was then stirred under a dry nitrogen atmosphere and heated to 55 °C. After 20 h, the resulting polymer (poly-L-**1**$_{100}$) was precipitated in a large amount of methanol, collected by centrifugation, and dried in vacuo at room temperature overnight (291 mg, 97% yield).

The obtained poly-L-**1**$_{100}$ (280 mg) was suspended in 100 mL of acetone, and the mixture was stirred at ambient temperature for 3 h. After filtration, the filtrate was evaporated to dryness under reduced pressure, giving *P*-poly-L-**1**$_{100}$(+) (40.0 mg, 14%). The acetone-insoluble polymer was dissolved in a small amount of $CHCl_3$, the solution was precipitated in a large amount of acetone, and the precipitate was then collected by filtration. After this procedure was repeated again, the *M*-poly-L-**1**$_{100}$(−) was obtained (178 mg, 64%).

In the same way, poly-L-**1**$_{50}$ ([**1**]/[**2**] = 50) was prepared by the polymerization of L-**1** with **2** in THF at 55 °C for 20 h, and *M*-poly-L-**1**$_{50}$(−) was obtained as the acetone-insoluble part from the poly-L-**1**$_{50}$.

Block Copolymerization of L-1, D-1, and Aib with *M*-poly-L-1$_{100}$(−), *P*-poly-L-1$_{100}$(+), and *M*-poly-L-1$_{50}$(−) as the Macroinitiator. A typical procedure is described below (see Scheme 3). *M*-poly-L-**1**$_{100}$(−) (20.0 mg), monomer D-**1** (20.0 mg, 55.8 mM), and a standard polystyrene (PSt, M_n = 2630, 44.0 mg) were placed in a dry ampule, which was then evacuated on a vacuum line and flushed with dry nitrogen. After the evacuation-flush procedure had been repeated three times, a three-way stopcock was attached to the ampule, and dry THF (0.56 mL) was added by a syringe. The mixture was then stirred under a dry nitrogen atmosphere and heated to 55 °C. The conversion of D-**1** was followed by measuring the SEC of the reaction mixture at appropriate time intervals. The peak area of the unreacted D-**1** relative to that of the internal standard

Scheme 3. Synthesis of Block Copolymers Initiated by *M*-poly-L-**1**$_{50}$(−), *M*-poly-L-**1**$_{100}$(−), and *P*-poly-L-**1**$_{100}$(+)

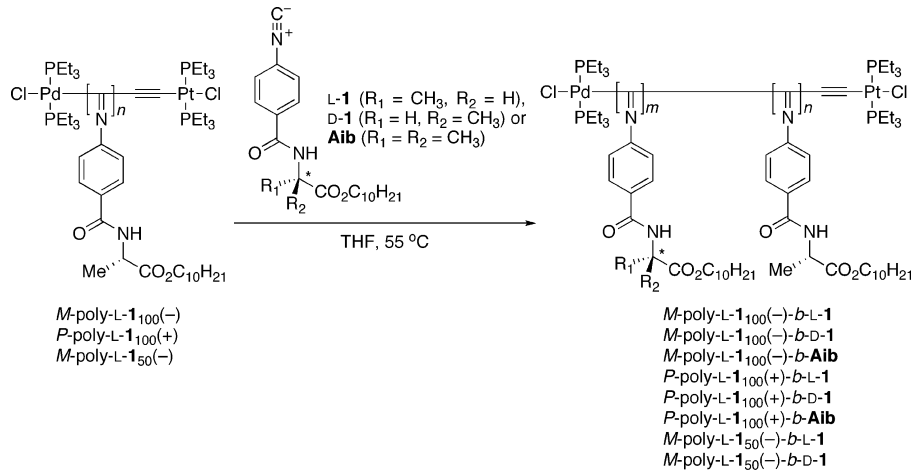

(PSt) was used for the determination of the conversion of D-**1** on the basis of the linear calibration curve. After the complete consumption of D-**1** was confirmed by SEC, the resulting copolymer (*M*-poly-L-**1**$_{100}$(−)-*b*-D-**1**) was precipitated in a large amount of methanol, collected by centrifugation, and dried overnight in vacuo at room temperature. To remove the PSt used as the internal standard, the methanol-insoluble part was dissolved in THF and reprecipitated in a large amount of acetone, collected by centrifugation, and dried overnight in vacuo at room temperature. In the same way, *M*-poly-L-**1**$_{100}$(−)-*b*-L-**1** and *M*-poly-L-**1**$_{100}$(−)-*b*-**Aib** were prepared using *M*-poly-L-**1**$_{100}$(−) as the macroinitiator. *P*-poly-L-**1**$_{100}$(+)-*b*-L-**1**, *P*-poly-L-**1**$_{100}$(+)-*b*-D-**1**, and *P*-poly-L-**1**$_{100}$(+)-*b*-**Aib** were also prepared by the copolymerization of L-**1**, D-**1**, and **Aib** with *P*-poly-L-**1**$_{100}$(+) as the macroinitiator, and *M*-poly-L-**1**$_{50}$(−)-*b*-L-**1** and *M*-poly-L-**1**$_{50}$(−)-*b*-D-**1** were obtained by the copolymerization of L-**1** and D-**1** with *M*-poly-L-**1**$_{50}$(−) as the macroinitiator.

Spectroscopic data of *M*-poly-L-**1**$_{100}$(−)-*b*-L-**1**, IR (KBr, cm^{-1}): 3278 (ν_{N-H}), 1749 ($\nu_{C=O}$ ester), 1634 (amide I), 1536 (amide II). ^{1}H NMR ($CDCl_3$, 55 °C): δ 0.86 (broad, CH_3, 3H), 1.25 (broad, CH_2, 14H), 1.53 (broad, CH_3 and CH_2, 5H), 4.08 (broad, CH_2, 2H), 4.50 (broad, CH, 1H), 4.9−7.2 (broad, aromatic, 4H), 7.9−8.8 (broad, NH, 1H). $[\alpha]^{25}_D$ −1936 (*c* 0.1, $CHCl_3$). Anal. Calcd for $(C_{21}H_{30}N_2O_3)_n$: C, 70.36; H, 8.44; N, 7.81. Found: C, 70.21; H, 8.39; N, 7.84.

Spectroscopic data of *M*-poly-L-**1**$_{100}$(−)-*b*-D-**1**, IR (KBr, cm^{-1}): 3273 (ν_{N-H}), 1749 ($\nu_{C=O}$ ester), 1634 (amide I), 1538 (amide II). ^{1}H NMR ($CDCl_3$, 55 °C): δ 0.86 (broad, CH_3, 3H), 1.25 (broad, CH_2, 14H), 1.52 (broad, CH_3 and CH_2, 5H), 4.08 (broad, CH_2, 2H), 4.49 (broad, CH, 1H), 4.9−7.4 (broad, aromatic, 4H), 7.9−9.0 (broad, NH, 1H). $[\alpha]^{25}_D$ −1423 (*c* 0.1, $CHCl_3$). Anal. Calcd for $(C_{21}H_{30}N_2O_3)_n$: C, 70.36; H, 8.44; N, 7.81. Found: C, 70.17; H, 8.17; N, 8.07.

Spectroscopic data of *M*-poly-L-**1**$_{100}$(−)-*b*-**Aib**, IR (KBr, cm^{-1}): 3287 (ν_{N-H}), 1742 ($\nu_{C=O}$ ester), 1634 (amide I), 1537 (amide II). ^{1}H NMR ($CDCl_3$, 55 °C): δ 0.86 (broad, CH_3), 1.25 (broad, CH_2), 1.53 (broad, CH_3 and CH_2), 4.08 (broad, CH_2), 4.50 (broad, CH), 4.9−7.2 (broad, aromatic), 7.9−8.8 (broad, NH). $[\alpha]^{25}_D$ −1903 (*c* 0.1, $CHCl_3$). Anal. Calcd for $(C_{43}H_{62}N_4O_6)_n$: C, 70.65; H, 8.55; N, 7.66. Found: C, 70.49; H, 8.54; N, 7.36.

Spectroscopic data of *P*-poly-L-**1**$_{100}$(+)-*b*-L-**1**, IR (KBr, cm^{-1}): 3263 (ν_{N-H}), 1749 ($\nu_{C=O}$ ester), 1635 (amide I), 1539 (amide II). ^{1}H NMR ($CDCl_3$, 55 °C): δ 0.87 (broad, CH_3, 3H), 1.26 (broad, CH_2, 14H), 1.54 (broad, CH_3 and CH_2, 5H), 4.04 (broad, CH_2, 2H), 4.44 (broad, CH, 1H), 4.8−7.2 (broad, aromatic, 4H), 8.2−8.8 (broad, NH, 1H). $[\alpha]^{25}_D$ +1767 (*c* 0.1, $CHCl_3$). Anal. Calcd for $(C_{21}H_{30}N_2O_3)_n$: C, 70.36; H, 8.44; N, 7.81. Found: C, 70.39; H, 8.67; N, 7.63.

Spectroscopic data of *P*-poly-L-**1**$_{100}$(+)-*b*-D-**1**, IR (KBr, cm^{-1}): 3273 (ν_{N-H}), 1749 ($\nu_{C=O}$ ester), 1635 (amide I), 1539 (amide II). ^{1}H NMR ($CDCl_3$, 55 °C): δ 0.88 (broad, CH_3, 3H), 1.26 (broad, CH_2, 14H), 1.55 (broad, CH_3 and CH_2, 5H), 4.07 (broad, CH_2, 2H), 4.45 (broad, CH, 1H), 4.8−7.4 (broad, aromatic, 4H), 8.2−8.8 (broad, NH, 1H). $[\alpha]^{25}_D$ +1901 (*c* 0.1, $CHCl_3$). Anal. Calcd for $(C_{21}H_{30}N_2O_3)_n$: C, 70.36; H, 8.44; N, 7.81. Found: C, 70.17; H, 8.47; N, 7.61.

Spectroscopic data of *P*-poly-L-**1**$_{100}$(+)-*b*-**Aib**, IR (KBr, cm^{-1}): 3274 (ν_{N-H}), 1747 ($\nu_{C=O}$ ester), 1635 (amide I), 1539 (amide II). ^{1}H NMR ($CDCl_3$, 55 °C): δ 0.87 (broad, CH_3), 1.26 (broad, CH_2), 1.55 (broad, CH_3 and CH_2), 4.02 (broad, CH_2), 4.61 (broad, CH), 4.9−7.2 (broad, aromatic), 7.4−9.0 (broad, NH). $[\alpha]^{25}_D$ +1845 (*c* 0.1, $CHCl_3$). Anal. Calcd for $(C_{43}H_{62}N_4O_6)_n$: C, 70.65; H, 8.55; N, 7.66. Found: C, 70.47; H, 8.49; N, 7.44.

Spectroscopic data of *M*-poly-L-**1**$_{50}$(−)-*b*-L-**1**, IR (KBr, cm^{-1}): 3274 (ν_{N-H}), 1748 ($\nu_{C=O}$ ester), 1635 (amide I), 1539 (amide II). ^{1}H NMR ($CDCl_3$, 55 °C): δ 0.86 (broad, CH_3, 3H), 1.26 (broad, CH_2, 14H), 1.53 (broad, CH_3 and CH_2, 5H), 4.05 (broad, CH_2, 2H), 4.50 (broad, CH, 1H), 4.9−7.2 (broad, aromatic, 4H), 8.0−8.8 (broad, NH, 1H). $[\alpha]^{25}_D$ −1875 (*c* 0.1, $CHCl_3$). Anal. Calcd for $(C_{21}H_{30}N_2O_3)_n$: C, 70.36; H, 8.44; N, 7.81. Found: C, 70.14; H, 8.58; N, 7.39.

Spectroscopic data of *M*-poly-L-**1**$_{50}$(−)-*b*-D-**1**, IR (KBr, cm^{-1}): 3273 (ν_{N-H}), 1748 ($\nu_{C=O}$ ester), 1635 (amide I), 1540 (amide II). ^{1}H NMR ($CDCl_3$, 55 °C): δ 0.86 (broad, CH_3, 3H), 1.26 (broad, CH_2, 14H), 1.53 (broad, CH_3 and CH_2, 5H), 4.08 (broad, CH_2, 2H), 4.51 (broad, CH, 1H), 4.8−7.2 (broad, aromatic, 4H), 8.0−9.0 (broad, NH, 1H). $[\alpha]^{25}_D$ −1699 (*c* 0.1, $CHCl_3$). Anal. Calcd for $(C_{21}H_{30}N_2O_3)_n$: C, 70.36; H, 8.44; N, 7.81. Found: C, 70.13; H, 8.63; N, 7.41.

SEC-MALS Measurements. The SEC-MALS measurements were carried out with THF containing 0.1 wt % TBAB used as the eluent at the flow rate of 0.5 mL/min. A standard polystyrene (M_w = 30 500 (Polymer Laboratories, Shropshire, U.K.)) was used to calculate the device constants, such as the interdetector delay, interdetector band broadening, and light scattering detector normalization. The polymers were completely dissolved in the eluent at the concentration of 0.1−0.2% (wt/vol) under gentle stirring for 1−2 h before injection. The evaluations of the molecular weights were accomplished using ASTRA V software (version 5.1.3.0). The d*n*/d*c* values of poly-L-**1**$_{100}$(−) and poly-L-**1**$_{100}$(+) in the eluent used for the evaluations were 0.1369 and 0.1367 mL/g, respectively, on the assumption that the d*n*/d*c* values were independent of the molecular weight.

AFM Measurements. Stock solutions of *M*-poly-L-**1**$_{100}$(−), *M*-poly-L-**1**$_{100}$(−)-*b*-L-**1**$_{100}$, *M*-poly-L-**1**$_{100}$(−)-*b*-D-**1**$_{100}$, *P*-poly-L-**1**$_{100}$(+), *P*-poly-L-**1**$_{100}$(+)-*b*-L-**1**$_{100}$, and *P*-poly-L-**1**$_{100}$(+)-*b*-D-**1**$_{100}$ in dry THF (0.02 mg/mL) were prepared. Samples for the AFM measurements were prepared by casting 20 μL aliquots of the stock solutions of the polymers. The casting was done at room temper-

ature on freshly cleaved HOPG under THF vapor atmospheres. After the polymers had been deposited on the HOPG, the HOPG substrates were further exposed to THF vapors for 2 h, and then the substrates were dried under vacuum for 2 h according to the reported procedure.[9,20] The organic solvent vapor was prepared by putting 1 mL of THF into a 2 mL flask that was inside a 50 mL flask, and the HOPG substrates were then placed in the 50 mL flask. The typical settings of the AFM for the high-magnification observations were as follows: amplitude 1.0−1.5 V; set point 0.9−1.4 V; scan rate 2.5 Hz. The Nanoscope image processing software was used for the image analysis.

Acknowledgment. We thank Dr. J. Kumaki and Dr. S.-i. Sakurai (JST) for helpful discussions and technical guidance in the AFM observations. This work was supported in part by a Grant-in-Aid for Scientific Research from the Japan Society for the Promotion of Science (JSPS), Japan Science and Technology Agency (JST), and the Global COE Program "Elucidation and Design of Materials and Molecular Functions" of the Ministry of Education, Culture, Sports, Science, and Technology, Japan. Z.-Q.W. thanks the JSPS for a postdoctoral fellowship for foreign researchers (no. P06350). K.N. expresses his thanks for a JSPS Research Fellowship for Young Scientists (no. 6683).

Supporting Information Available: SEC chromatograms for the block copolymerizations of L-**1** and D-**1** initiated by *P*-poly-L-$\mathbf{1}_{100}(+)$ and *M*-poly-L-$\mathbf{1}_{50}(-)$, IR spectra of *M*-poly-L-$\mathbf{1}_{100}(-)$, *M*-poly-L-$\mathbf{1}_{100}(-)$-*b*-L-**1**, and *M*-poly-L-$\mathbf{1}_{100}(-)$-*b*-D-**1** in $CHCl_3$, plots of M_n values versus the number-average molecular length (L_n) observed by AFM measurements, and AFM phase images of 2D self-assembled *P*-poly-L-$\mathbf{1}_{100}(+)$-*b*-L-**1**, *P*-poly-D-$\mathbf{1}_{100}(+)$-*b*-D-**1**, *M*-poly-L-$\mathbf{1}_{100}(-)$-*b*-L-**1**, and *M*-poly-L-$\mathbf{1}_{100}(-)$-*b*-D-**1** on HOPG. This material is available free of charge via the Internet at http://pubs.acs.org.

JA900036N